HHS Public Access

Author manuscript

Nat Genet. Author manuscript; available in PMC 2020 April 28.

Published in final edited form as:

Nat Genet. 2019 November ; 51(11): 1580–1587. doi:10.1038/s41588-019-0514-8.

HDAC9 is implicated in atherosclerotic aortic calcification and affects vascular smooth muscle cell phenotype

Rajeev Malhotra[1,2,35], Andreas C. Mauer[1], Christian L. Lino Cardenas[1,2], Xiuqing Guo[3], Jie Yao[3], Xiaoling Zhang[4,5], Florian Wunderer[6,7], Albert V. Smith[8,9], Quenna Wong[10], Sonali Pechlivanis[11], Shih-Jen Hwang[4,12], Judy Wang[13], Lingyi Lu[14], Christopher J. Nicholson[1], Georgia Shelton[1], Mary D. Buswell[1], Hanna J. Barnes[1], Haakon H. Sigurslid[1], Charles Slocum[1], Caitlin O'Rourke[1], David K. Rhee[1,2], Aranya Bagchi[2,6], Sagar U. Nigwekar[2,15], Emmanuel S. Buys[2,6], Catherine Y. Campbell[16], Tamara Harris[17], Matthew Budoff[18], Michael H. Criqui[19], Jerome I. Rotter[3], Andrew D. Johnson[4,12], Ci Song[4,12,20], Nora Franceschini[21], Stephanie Debette[22], Udo Hoffmann[2,23], Hagen Kälsch[24,25], Markus M. Nöthen[26,27], Sigurdur Sigurdsson[8], Barry I. Freedman[14], Donald W. Bowden[14], Karl-Heinz Jöckel[11], Susanne Moebus[11,28], Raimund Erbel[11], Mary F. Feitosa[13], Vilmundur Gudnason[8,29], George Thanassoulis[4,30], Warren M. Zapol[2,6], Mark E. Lindsay[1,2], Donald B. Bloch[2,6,31,34], Wendy S. Post[32,34], Christopher J. O'Donnell[1,4,33,34,35]

[1]Division of Cardiology, Department of Medicine, Massachusetts General Hospital, Boston, MA, USA [2]Harvard Medical School, Boston, MA, USA [3]Institute for Translational Genomics and Population Sciences, Los Angeles Biomedical Research Institute and Department of Pediatrics, Harbor-UCLA Medical Center, Torrance, CA, USA [4]National Heart Lung and Blood Institute's Framingham Heart Study, Framingham, MA, USA [5]Departments of Medicine (Biomedical Genetics) and Biostatistics, Boston University Schools of Medicine and Public Health, Boston, MA, USA [6]Department of Anesthesia, Critical Care, and Pain Medicine, Massachusetts General Hospital, Boston, MA, USA [7]Department of Anesthesiology, Intensive Care Medicine and Pain Therapy, University Hospital Frankfurt, Frankfurt am Main, Germany [8]Icelandic Heart Association, Kopavogur, Iceland [9]Department of Biostatistics, University of Michigan, Ann Arbor, MI, USA [10]Department of Biostatistics, University of Washington, Seattle, WA, USA [11]Institute for Medical Informatics, Biometry and Epidemiology, University Hospital Essen, Essen, Germany [12]National

[35] These authors jointly directed this work. Correspondence should be addressed to R.M. (rmalhotra@mgh.harvard.edu) or C.J.O. (Christopher.ODonnell@va.gov).

Author Contributions

Concept and design of genome-wide association study: R.M., A.C.M., X.G., J.Y., C.Y.C., W.S.P., C.J.O.

Cohort-based phenotype and genotype acquisition: A.V.S., Q.W., S.P., S.-J.H., J.W., L.L., C.Y.C., T.H., M.B., M.H.C., J.I.R., A.D.J., C. Song, N.F., S.D., U.H., H.K., M.M.N., S.S., B.I.F., D.W.B., K.-H.J., S.M., R.E., M.F.F., V.G., G.T., W.S.P., C.J.O.

Meta-analysis and sQTL analysis: R.M., A.C.M., X.G., J.Y., X.Z., W.S.P., C.J.O.

Concept and design of cell-based assays and *in vivo* studies: R.M.

Acquisition, analysis, or interpretation of data in cell-based assays and *in vivo* studies: R.M., C.L.L.C., F.W., C.J.N., G.S., M.D.B., H.J.B., C. Slocum, H.H.S., C.O., D.K.R., A.B., S.U.N., E.S.B., W.M.Z., M.E.L., D.B.B.

Drafting of the manuscript: R.M., A.C.M., C.J.O.

Critical revision of the manuscript for important intellectual content: all authors

Approval of content of manuscript: all authors

Competing Interests

R.M. serves as a consultant for MyoKardia and Third Pole. A.B. is a consultant for Lungpacer Medical, Inc. U.H. is a consultant for Abbott, Duke University (NIH), and Recor Medical.

Heart, Lung and Blood Institute, Population Sciences Branch, Division of Intramural Research, Bethesda, MD, USA [13]Division of Statistical Genomics, Washington University School of Medicine, St. Louis, MO, USA [14]Wake Forest School of Medicine, Winston-Salem, NC, USA [15]Division of Nephrology, Department of Medicine, Massachusetts General Hospital, Boston, MA, USA [16]Mid-Atlantic Permanente Medical Group, Rockville, MD, USA [17]National Institute on Aging, Bethesda, MD, USA [18]Division of Cardiology, Department of Medicine and Los Angeles Biomedical Research Institute, Harbor-UCLA Medical Center, Torrance, CA, USA [19]Department of Family Medicine and Public Health, University of California, San Diego, La Jolla, CA, USA [20]Deptartment of Medical Sciences, Uppsala University, Uppsala, Sweden [21]Department of Epidemiology, University of North Carolina, Chapel Hill, NC, USA [22]Inserm U1219, University of Bordeaux, and Department of Neurology at Bordeaux University Hospital, Bordeaux, France [23]Department of Radiology, Massachusetts General Hospital, Boston, MA, USA [24]Department of Cardiology, Alfried Krupp Krankenhaus, Essen, Germany [25]Witten/Herdecke University, Witten, Germany [26]Institute of Human Genetics, University of Bonn, Bonn, Germany [27]Department of Genomics, Life & Brain GmbH, University of Bonn, Bonn, Germany [28]Centre for Urban Epidemiology, University Hospital Essen, Essen, Germany [29]Faculty of Medicine, University of Iceland, Reykjavik, Iceland [30]Department of Medicine, McGill University Health Center, Montreal, Quebec, Canada [31]Division of Rheumatology, Department of Medicine, Massachusetts General Hospital, Boston, MA, USA [32]Division of Cardiology, Department of Medicine, Johns Hopkins University, Baltimore, MD, USA [33]US Department of Veterans Affairs, Boston, MA, USA [34]These authors contributed equally to this work.

Abstract

Aortic calcification is an important independent predictor of future cardiovascular events. We performed a genome-wide association meta-analysis to determine single nucleotide polymorphisms (SNPs) associated with the extent of abdominal (AAC, $n = 9,417$) or descending thoracic (TAC, $n = 8,422$) aortic calcification. Two genetic loci, *HDAC9* and *RAP1GAP*, were associated with AAC at a genome-wide level ($P < 5.0 \times 10^{-8}$). No SNPs were associated with TAC at the genome-wide threshold. Increased expression of HDAC9 in human aortic smooth muscle cells (HASMCs) promoted calcification and reduced contractility, while inhibition of HDAC9 in HASMCs inhibited calcification and enhanced cell contractility. In matrix Gla protein (MGP)-deficient mice, a model of human vascular calcification, mice lacking HDAC9 had a 40% reduction in aortic calcification and improved survival. This translational genomic study identifies the first genetic risk locus associated with calcification of the abdominal aorta and describes a novel role for HDAC9 in the development of vascular calcification.

Editorial summary

Genome-wide analyses identify variants near *HDAC9* associated with abdominal aortic calcification and other cardiovascular phenotypes. Functional work shows that HDAC9 promotes an osteogenic vascular smooth muscle cell phenotype, enhancing calcification and reducing contractility.

Arterial wall calcification is a hallmark of atherosclerosis and serves as an important factor for cardiovascular (CV) risk assessment[1,2]. Although studies have identified the genetic underpinnings of coronary artery calcification[3,4] and valvular calcification[5], the genetic determinants of human aortic calcification remain unknown. As with coronary artery calcification, both abdominal aortic calcification and thoracic aortic calcification are strong independent predictors of CV-related events and death[6–8]. A meta-analysis of studies of the CVD risk conferred by AAC found that individuals with the highest, compared to the lowest, tertile of AAC had a relative risk of 1.92 for coronary events and of 1.56 for cerebrovascular events[9]. Higher levels of AAC were associated with a >75% increase in CV mortality[10]. Aortic calcification is also associated with aortic aneurysms[11] as well as maladaptive cardiac responses, such as left ventricular hypertrophy and diastolic dysfunction, caused by arterial stiffening[12–14].

Identifying the genetic determinants of abdominal and thoracic aortic calcification may help elucidate novel mechanisms underlying vascular disease. We therefore performed a genome-wide association study (GWAS) meta-analysis of cohorts within the Cohorts for Heart and Aging Research in Genome Epidemiology (CHARGE) consortium[15]. Subsequent association analyses were performed in multi-ethnic cohorts to validate genome-wide significant findings.

Individuals of European ancestry from five different cohorts (Framingham Heart Study, FHS; Age, Gene-Environment Susceptibility-Reykjavik Study, AGES-RS; Multi-Ethnic Study of Atherosclerosis, MESA; Family Heart Study, FamHS; and Heinz Nixdorf Recall study, HNR) were included in the discovery analysis. Baseline characteristics of the participants in the discovery analysis are provided in Supplementary Table 1. Quantification of the degree of vascular calcification from computed tomography (CT) scans was available for the abdominal aorta in 9,417 participants and for the descending thoracic aorta in 8,422 participants. The validation stage of the study used data obtained from non-European ancestry groups in MESA (African American, $n = 343$; Hispanic American, $n = 496$), FamHS (African American, $n = 621$), and the African American-Diabetes Heart Study (AA-DHS, $n = 750$).

The genomic inflation factor (λ) in the discovery meta-analysis was small for both AAC ($\lambda = 1.09$) and TAC ($\lambda = 1.00$), suggesting that potential genotyping artifact, cryptic relatedness in the population, or systematic differences in allelic distributions due to population stratification did not cause significant bias[16]. The quantile-quantile plots for the AAC and TAC meta-analyses (Fig. 1a and Supplementary Fig. 1, respectively) demonstrated that the observed distribution of *P* values for both vascular phenotypes matched the expected distribution.

SNPs associated with AAC were identified in two genetic loci (Fig. 1a–c and Table 1), the first encoding histone deacetylase 9 (*HDAC9,* hg38 chr7:18,086,949–18,666,929) and the second encoding RAP1 GTPase activating protein (*RAP1GAP,* hg38 chr1:21,596,221–21,669,306). SNPs associated at a genome-wide significance level with AAC in the *HDAC9* locus were rs57301765, rs2107595, rs28688791, rs2023936, rs2526620, and rs7798197 (Table 1). SNPs associated with AAC in the *RAP1GAP* locus included rs4654975 and

rs3767120; two additional SNPs (rs10159452 and rs10157126) were just below the threshold for genome-wide significance ($P = 5.8–5.9 \times 10^{-8}$). All of the SNPs associated with AAC are located in non-coding regions of their respective gene loci. The minor allele at each SNP was associated with a greater degree of AAC (Table 1), and both the magnitude and direction of association were consistent across all discovery stage cohorts (one representative SNP from each locus is highlighted in Supplementary Table 2). Additional SNPs ($n = 14$) with suggestive evidence for association with AAC ($P < 1 \times 10^{-6}$) are listed in Supplementary Table 3.

No SNPs were found to be associated with TAC at a genome-wide level of significance. There was evidence for borderline significance ($P = 8.6 \times 10^{-8}$) for one SNP on chromosome 9 (rs58674255) in the vacuolar protein sorting 13 homolog A (*VPS13A*) locus (Table 1 and Supplementary Fig. 1). Additional SNPs ($n = 22$) with suggestive evidence for association ($P < 1 \times 10^{-6}$) are listed in Supplementary Table 4.

SNPs that were associated with AAC in the discovery analysis were tested for association in independent validation cohorts. All six SNPs in the *HDAC9* locus were significantly associated with AAC in an independent replication sample from MESA consisting of Hispanic Americans ($n = 496$, all $P < 1.9 \times 10^{-4}$), and exhibited the same direction of association as the discovery cohorts (Table 2). Of these six SNPs, rs2107595 demonstrated the strongest association with a Z score of 4.7 ($P = 2.8 \times 10^{-6}$). The two SNPs in the *RAP1GAP* locus were not associated with AAC in the MESA Hispanic-American cohort (Table 2).

There was a modest association between rs2107595 and AAC in African Americans from the FamHS ($n = 621$, $Z = 2.5$, $P = 0.01$), with a direction of association consistent with the discovery analysis. However, no significant association between SNPs from the *HDAC9* locus and AAC was observed in the MESA African-American cohort ($n = 343$) or the AA-DHS ($n = 631$), or in a meta-analysis combining these three cohorts ($Z = 1.41$, $P = 0.12$; Supplementary Table 5). There was no association between SNPs in the *RAP1GAP* locus and AAC in the African-American cohorts, although there was limited power to detect an association given the small sample sizes of the populations.

To assess whether the genetic determinants of AAC are similar to that of calcification in other vascular beds and for cardiovascular disease, we determined whether the SNPs associated with AAC were also associated with TAC ($n = 8,422$), coronary artery calcification (in the CHARGE Consortium, $n = 9,992$)[3], carotid artery plaque (in the CHARGE Subclinical Atherosclerosis consortium, $n = 40,574$, unpublished data), and clinically apparent coronary heart disease (in the CardiogramPlusC4D Consortium, $n = 193,189$)[17]. All six SNPs in the *HDAC9* locus met the genome-wide level of significance for association with myocardial infarction, with the strongest association for rs2107595 ($P = 8.1 \times 10^{-11}$, Supplementary Table 6). rs57301765 was nominally associated with TAC ($P = 0.047$), while rs2107595 was associated with coronary artery calcification ($P = 0.039$). Similar to the findings from a previous analysis within the CHARGE consortium of genetic association with carotid artery plaque using HapMap ($n = 25,179$, $P = 1.8 \times 10^{-3}$)[18], all six SNPs in the *HDAC9* locus were associated with the presence of carotid artery plaque in a

larger sample size using 1000G imputation[19], with the strongest association for rs2107595 ($P = 7.8 \times 10^{-4}$, Supplementary Table 6). We therefore conclude that SNPs in the *HDAC9* locus may also be associated with vascular disease in the thoracic aorta, coronary arteries, and carotid arteries. Previous GWAS have found associations between *HDAC9* and large vessel ischemic stroke and myocardial infarction[17,20,21]. Interestingly, other SNPs previously known to be associated with stroke, myocardial infarction, or coronary artery disease at the genome-wide level[22] had significantly weaker associations with AAC ($P > 10^{-3}$, Supplementary Table 7) compared to the SNPs in the *HDAC9* locus, further implicating HDAC9 specifically in the development of abdominal aortic calcification. Splicing quantitative trait loci (sQTL) analyses indicated that some minor alleles in the *HDAC9* locus that are associated with increased AAC are also associated with increased expression of certain splicing transcripts of *HDAC9* (Supplementary Note).

The acetylation and deacetylation of histones serves as a key determinant of chromatin structure and gene transcription and allow for the coupling of extracellular signals with genomic architecture[23]. Histone deacetylases remove acetyl groups from histones and consist of a superfamily of eleven enzymes that are further subdivided into four families (HDAC class I, IIa, IIb, and IV)[24]. HDAC9 belongs to the class IIa HDAC family[25]. To examine the role of HDAC9 in vascular calcification, human aortic smooth muscle cells (HASMCs) were treated with calcifying media in the presence or absence of TMP269, a class IIa HDAC inhibitor[26]. Compared to HASMCs incubated in normal tissue culture medium, HASMCs treated with calcifying medium for 10 days exhibited a >2-fold increase in mRNA levels of *RUNX2*, a master regulator of osteogenic phenotype switch in vascular SMCs (Fig. 2a)[27]. Treatment of HASMCs with TMP269 prevented induction of *RUNX2* expression in response to calcifying medium, and TMP269-treated HASMCs incubated in calcifying medium had reduced calcification (Fig. 2a,b). Because TMP269 inhibits all of the members in the HDAC class IIa family, we next sought to determine whether specific knockdown of *HDAC9* mRNA levels with siRNA (siHDAC9) was sufficient to inhibit *RUNX2* gene induction and *in vitro* calcification of HASMCs incubated in calcifying media. Compared to the effects of control siRNA (siCTRL), siHDAC9 decreased *HDAC9* mRNA levels by >75%, decreased *RUNX2* expression by >50% (Fig. 3a,b), and reduced the *in vitro* calcification of HASMCs treated with calcifying medium (Fig. 3c).

The observation that inhibition of HDAC9 activity reduces *RUNX2* expression implicates HDAC9 in the development of an osteogenic vascular SMC phenotype, which is associated with reduced contractility and increased proliferation[28]. Therefore, we hypothesized that inhibition of *HDAC9* gene expression would increase contractility and reduce proliferation of vascular SMCs. Treatment of HASMCs with siHDAC9 increased contractility by ~30% ($P = 0.009$) as measured using a cell-embedded collagen gel contraction assay (Fig. 3d)[29]. Furthermore, HASMCs treated for 2 days with siHDAC9 exhibited a ~60% reduction in proliferation (Fig. 3e). These results indicate that inhibition of HDAC9 expression favors an increased contractile and decreased proliferative vascular smooth muscle cell phenotype.

To determine whether increased expression of HDAC9 promotes an osteogenic vascular SMC phenotype, we treated HASMCs with an adenoviral vector expressing *HDAC9*. Treatment of HASMCs with the *HDAC9* adenovirus resulted in a 75% increase in *RUNX2*

mRNA after 8 days of treatment (Fig. 3f) and resulted in increased calcification (Fig. 3g). Furthermore, treatment of HASMCs with *HDAC9* adenovirus reduced contractility (Fig. 3h). Taken together, these results indicate that increased HDAC9 expression promotes a vascular SMC osteogenic phenotype and calcification, and inhibition or decreased levels of HDAC9 reduces *RUNX2* gene expression and decreases the calcification of HASMCs.

We used a mouse model of vascular calcification caused by matrix Gla protein (MGP) deficiency[30] to investigate the role of HDAC9 in vascular calcification *in vivo*, as detailed in the Supplementary Note. Compared to $Mgp^{-/-}$ $Hdac9^{+/+}$ mice, $Mgp^{-/-}$ $Hdac9^{-/-}$ mice exhibited a ~50% reduction in aortic *Runx2* mRNA levels ($P = 0.024$) associated with reduced disruption of elastin fibers, a ~40% reduction in aortic calcification as assessed by near-infrared fluorescent imaging ($P = 0.027$), and improved survival (Fig. 4a–g and Supplementary Fig. 2). Furthermore, primary aortic SMCs isolated from $Hdac9^{-/-}$ mice had reduced expression of osteogenic markers and were protected from calcification (Supplementary Fig. 3). These results identify HDAC9 as an important contributor to the development of vascular calcification *in vivo*.

In summary, we performed a GWAS with over 9,400 participants and identified a novel genetic locus associated with abdominal aortic calcification, a strong and independent predictor of cardiovascular disease events. Multiple SNPs in the *HDAC9* locus were associated with AAC. The association between SNPs in the *HDAC9* locus and AAC was validated in an independent cohort of Hispanic Americans. These SNPs in the *HDAC9* locus were associated with other forms of calcification, including thoracic aortic and coronary artery calcification. Reducing the expression of HDAC9 or inhibiting its activity prevented the *in vitro* calcification of HASMCs. Furthermore, vascular calcification was significantly reduced and survival improved in $Mgp^{-/-}$ mice deficient in HDAC9.

Previous GWAS found an association between *HDAC9* and large vessel ischemic stroke, myocardial infarction, and increased pulse pressure[17,20,21,31]. There is also a strong clinical link between aortic calcification and these indicators of cardiovascular disease[7,32,33]. Our identification of HDAC9 as an activator of vascular calcification therefore offers a potential unifying molecular mechanism for the associations of *HDAC9* with stroke, myocardial infarction, and pulse pressure. Vascular calcification is characterized by the phenotypic transition of vascular smooth muscle cells to osteoblast-like cells that deposit calcium phosphate in the extracellular space[28,34,35]. RUNX2 is a master regulator of this osteogenic phenotypic change[36,37], which is marked by an increase in vascular smooth muscle cell proliferation and reduced cell contractility[38]. In this study, inhibition of HDAC9 in HASMCs prevented calcification induced by calcifying medium. In addition, inhibition of HDAC9 reduced RUNX2 expression, decreased cell proliferation, and increased cell contractility. Conversely, adenoviral-mediated expression of HDAC9 in HASMCs promoted osteogenic phenotype switch and calcification. The results of these functional assays underscore an important role for HDAC9 in altering the phenotypic state of vascular smooth muscle cells. Further investigation is warranted to determine whether HDAC9 contributes to the pathogenesis of a wide range of vascular smooth muscle cell-associated diseases, including hypertension, arterial stiffness, and aneurysmal disease[21,39] in addition to

coronary artery disease and stroke. There are potential limitations to our study, as described in the Supplementary Note.

In conclusion, in this translational genomic study, we identified a novel association between variants in the *HDAC9* locus and AAC. Functional studies implicate HDAC9 as an important determinant of vascular smooth muscle cell phenotype and calcification. Deficiency of HDAC9 significantly decreased vascular calcification in a mouse model. This study is the first to identify a genetic risk locus associated with calcification of the abdominal aorta and describes a novel role for HDAC9 in the development of vascular calcification. Our findings highlight HDAC9 as a potential target of therapy for vascular calcific disease.

Methods

Study design

The Cohorts for Heart and Aging Research in Genomic Epidemiology (CHARGE) Consortium is an ongoing investigator-driven collaboration among several large, population-based cohort studies that have genome-wide genotype data in addition to comprehensive individual phenotyping for a variety of endpoints. Details of this collaboration have been described previously[5,15]. We employed a two-stage analysis to first discover and then validate the association of genetic loci with the extent of abdominal aortic calcification (AAC) and thoracic aortic calcification (TAC). The initial discovery meta-analysis included genome-wide association study (GWAS) data from five large population-based cohorts including the Framingham Heart Study (FHS), the Age, Gene-Environment Susceptibility-Reykjavik Study (AGES-RS), the Multi-Ethnic Study of Atherosclerosis (MESA), the Family Heart Study (FamHS), and the Heinz Nixdorf Recall (HNR) study. Discovery cohort participants were of White European ancestry and had undergone genotyping and computed tomography (CT) scanning to assess the presence of, and to quantify, AAC and TAC.

In stage 2, significant findings from this initial meta-analysis were tested in additional multi-ethnic cohorts, including African American and Hispanic American participants from MESA, the FamHS, and the African-American Diabetes Heart Study (AA-DHS).

All cohorts obtained approval from their institutional review board to perform the study and individual participant informed consent was obtained. Further details about the discovery and validation cohorts are described in the Supplementary Note.

Assessment of aortic calcium

A similar methodology for assessing aortic calcium was used in each of the cohorts, according to established standards. Calcium strongly attenuates x-rays, appears bright on CT scans, and is readily differentiated from surrounding tissue. Using standard Agatston methodology[40], a threshold of ≥3 contiguous pixels of ≥130 Hounsfield units brightness was used to define calcium in FHS, MESA, FamHS, and AA-DHS, and ≥4 pixels was required in HNR. A volume-based approach to calcium measurement was used in AGES-RS and a calcium mass score was used in AA-DHS. Agatston score, volumetric assessment, and mass score of calcium are widely used and are highly correlated with one another[2,41]. While

individual cohorts used different scanner types, ranging from EBCT to 8-slice MDCT, the equivalency of various scanner types and protocols for the detection and quantification of calcium has been demonstrated previously[42–44]. Additionally, all sites used calcium phantoms to enhance quality control during image acquisition and analysis.

Statistical analyses

Discovery and replication analyses—For the discovery stage (stage 1), the association between each SNP and the extent of AAC and TAC was analyzed in each individual cohort independently, using linear regression with adjustments for age, sex, and ancestry (if necessary). Both AAC and TAC were analyzed as continuous variables using the log transformation of (calcium score + 1). GEE was used in the FHS analyses to account for familial correlations. While the FHS, AGES-RS, MESA, and FamHS cohorts provided data for AAC, the FHS, AGES-RS, MESA, and HNR cohorts provided data for TAC (Supplementary Table 1).

Individual study results were combined using fixed effects meta-analysis as implemented in the METAL software[45]. Given the unequal number of cases and controls in each study, we utilized the effective sample size as the weighting scheme. This weighting approach also provides the flexibility to allow for different β-coefficients and standard errors from individual studies that utilize different measurement units, such as the volumetric scoring in AGES-RS compared to the Agatston score in the other discovery cohorts. Heterogeneity analysis was also performed with no evidence of heterogeneity found between studies. Study-specific results were genomic control corrected, and SNPs with minor allele frequency <0.01 or an imputation ratio <0.3 were excluded prior to meta-analysis. Meta-analysis results were filtered to ensure that ≥2 cohorts contributed to the statistics for each SNP. For additional quality assessment, quantile-quantile (Q-Q) plots of the distribution of observed versus predicted p-values were created as were Manhattan plots of the SNP *P*-values of association relative to the SNP chromosomal location (Fig. 1a and Supplementary Fig. 1). To limit the number of false-positive associations given the large number of analyzed SNPs, the threshold for statistical genome-wide significance for individual SNP results in the discovery analysis was defined *a priori* as $P < 5.0 \times 10^{-8}$, as is standard for GWAS. SNPs with $P < 1.0 \times 10^{-6}$ are also reported as these may generate hypotheses for future studies (Supplementary Tables 2 and 3).

Assessment of SNPs for validation study—In the validation stage, the SNPs that met genome-wide significance in the discovery analysis were tested in additional cohorts, including a multi-ethnic population from MESA, FamHS, and the AA-DHS. As eight SNPs were tested for the validation phase, statistical significance was defined using the conservative Bonferroni correction as $P < 0.05/8 = 0.0062$, with a consistent direction of association.

Splicing quantitative trait loci (sQTL) analyses—The sQTL analyses were conducted using two expression datasets available in the Framingham Heart Study (FHS). Firstly, we analyzed 5,257 FHS participants with both 1000G-imputed SNP data and whole blood Affymetrix Exon Array expression data by following the same analytic pipeline, as

previously described[46]. Secondly, using whole blood RNA-sequencing data available for 183 FHS participants, we applied Altrans (Ongen et al. doi: http://dx.doi.org/10.1101/014126) to identify significant associations between Ensembl transcripts and SNPs.

Functional and *in vivo* studies

Animals—This study was carried out in strict accordance with the recommendations in the Guide for the Care and Use of Laboratory Animals of the National Institutes of Health. Housing and all procedures involving mice described in this study were specifically approved by the Institutional Animal Care and Use Committees of Massachusetts General Hospital (Subcommittee on Research Animal Care, protocol #2008N000169). *Mgp*$^{+/-}$ mice were generated by G. Karsenty and colleagues[30]. *Hdac9*$^{-/-}$ mice were generated by E. Olson and colleagues[47]. To investigate the role of HDAC9 in vascular calcification in MGP-deficient mice, *Mgp*$^{+/-}$ mice were mated with *Hdac9*$^{-/-}$ mice to generate *Mgp*$^{-/-}$ *Hdac9*$^{-/-}$ mice. Animals were maintained on a standard diet. Survival studies were performed and the Kaplan-Meier statistic with log-rank testing was used to compare survival of mice.

Calcification of HASMCs—HASMCs were obtained from Cell Applications (#355–75a). To induce calcification in HASMCs, cells were treated with DMEM supplemented with 10% fetal bovine serum, 10 mM β-glycerophosphate disodium, 50 μg/mL L-ascorbic acid, and 10 nM dexamethasone, as previously described[48]. To assess the effects of HDAC9 inhibition on calcification, cells were treated with either 100 nM TMP269 (Selleckchem, Cat No. S7324) or vehicle (DMSO) control. Media and treatment were replenished every 24 hours for 7–10 days. Either RNA was isolated from cells to assess mRNA levels (see below) or the cells were fixed in 10% formalin and incubated with Alizarin Red or von Kossa stain to detect calcification. For Alizarin Red staining, cells were treated with a 2% Alizarin Red solution (pH 4.1–4.3) for 20 minutes, followed by multiple washes with distilled water. For von Kossa staining, cells were incubated in 5% silver nitrate solution and exposed to a 100 Watt bulb for 1–2 hours. Removal of unreacted silver was performed by subsequent treatment with 5% sodium thiosulfate. Cells were then washed with distilled water.

siRNA-mediated knockdown and adenovirus-mediated expression of HDAC9—siRNA directed against *HDAC9* (siHDAC9) and scrambled control siRNA (siCTRL) were obtained from Dharmacon (SMARTpool, Thermo Scientific). HASMCs were transfected with siRNA using Lipofectamine RNAiMAX reagent, as described by the manufacturer (Life Technologies).

Recombinant adenoviruses expressing either human wild-type HDAC9 (NM_058176) with a C-terminal Enhanced Green Fluorescent Protein (eGFP) tag or expressing eGFP alone were obtained from Vector Biolabs (human adenovirus type 5 [dE1/E3], promoter: cytomegalovirus, Catalog #1768, Malvern, PA). HASMCs were transduced with the adenovirus vectors in regular growth medium. After 24 hours, cells expressing eGFP were detected using fluorescent microscopy. RNA and protein levels were analyzed by qPCR and Western blot, respectively, 8 days after transduction.

Proliferation assay—HASMCs were plated in a 96-well format and transfected with either siHDAC9 or siCtrl for 48 hours. An MTT (3-(4,5-dimethylthiazol-2-yl)-2,5-diphenyltetrazolium bromide)-based assay (ATCC #30–1010K) was used to assess cell proliferation. Briefly, 10 μL of the MTT reagent was added to each well, and the plate was incubated at 37 °C in a cell culture incubator in the dark for 3 hours, until a purple precipitate was visible inside the cells using standard light microscopy. Detergent reagent (100 μL) was then added to each well, and the plate was incubated at room temperature in the dark for 2 hours before measurement of absorbance at 570 nm.

Collagen matrix cell contraction assay—HASMC contraction was measured by the extent of deformation of collagen lattices, as previously described[49]. Cells were treated with siRNA for 24 hours prior to being embedded in collagen matrices, per manufacturer's protocol (Cell Contraction Assay #CBA-201, Cell Biolabs, Inc). After 48 hours, the collagen lattice was released from the culture dish. Upon releasing the collagen lattice, the embedded cells are free to contract the deformable collagen lattice, resulting in a reduction of the lattice surface area. After detachment of the collagen gel lattice from the dish, changes in the gel surface area were quantified using Image J software.

Near-infrared imaging and quantification of aortic calcification—Age-matched wild-type, *Mgp*$^{-/-}$ *Hdac9*$^{+/+}$, *Mgp*$^{-/-}$ *Hdac9*$^{+/-}$, and *Mgp*$^{-/-}$ *Hdac9*$^{-/-}$ mice were injected via the tail vein with OsteoSense-680 (PerkinElmer, 5 μl/g each) 24 hours before euthanasia, as described previously[50,51]. Aortas were isolated and analyzed *ex vivo* by fluorescence reflectance imaging using an Odyssey Imaging System (LI-COR Biotechnology, Lincoln, NE) and software version 3.0.16[52,53].

Aortic immunofluorescence and histology—Aortas were embedded and cryopreserved in optimal cutting-temperature medium (Sakura Tissue-Tek, Zoeterwoude, Netherlands), and 6-μm sections were prepared[54]. To detect HDAC9 in aortas, frozen tissue sections were fixed in cold 100% methanol and incubated with primary antibody (Abcam, #ab59718) specific for a 50-kDa isoform of HDAC9. To determine the association between HDAC9 expression and the expression of other HDACs as well as contractile and extracellular matrix degradation markers, sections were also treated with antibodies for HDAC4 and HDAC7 (Abcam, #ab12171 and ab50212, respectively), SM22α, MYH11 and MMP9 (Abcam: #ab14106, ab53219, and ab38898). The location of nuclei was identified by staining with 4',6-diamidino-2-phenylindole (DAPI). Two-dimensional and white light images were analyzed using Image J software. Aortas were also fixed in formalin (10%) for 24 hours prior to paraffinization and sectioning (6 μm). Staining with Verhoeff-Van Gieson (Thermo Scientific, MI, USA) was performed for assessment of elastin integrity.

Immunoblot techniques—HASMCs and aortas were homogenized in RIPA buffer containing protease and phosphatase inhibitors (Sigma). Lysates (20 μg/lane) were mixed with denaturing buffer (1× Laemmli loading buffer with 10% of β-mercaptoethanol) and analyzed by SDS–PAGE/Western. Rabbit polyclonal anti-HDAC9 antibodies were used to detect the 125-kDa isoform of human HDAC9 in HASMCs (Origene, TA318928). Rabbit polyclonal antibodies directed against the murine short isoform of HDAC9 (MITR) were

used to detect HDAC9 protein in mouse aortas (Abcam, #ab59718). Rabbit polyclonal antibodies directed against glyceraldehyde 3-phosphate dehydrogenase (GAPDH, Cell Signaling #2118) were used to detect GAPDH protein. Blots were incubated with fluorescent-dye labeled anti-rabbit IgG IRDye 800CW (LI-COR, Lincoln, NE) and protein bands were imaged using a LI-COR Odyssey detection system (LI-COR, Lincoln, NE).

Preparation of mouse aortic vascular smooth muscle cells—Vascular smooth muscle cells (VSMCs) were isolated from aortas of *Hdac9*$^{-/-}$ mice and wild-type littermate controls, as previously described[48,55]. Aortas were digested with Type 2 collagenase (175 U/mL, Worthington) and elastase (1.25 U/mL, Sigma) for 30 minutes, and the adventitial layer was removed. Aortas were further digested with collagenase and elastase for 60 minutes, and cells were plated and maintained in Dulbecco's Minimum Essential Medium (DMEM, Invitrogen) supplemented with 10% fetal bovine serum (FBS, Invitrogen), 100 units/ml of penicillin, and 100 μg/ml of streptomycin at 37°C with 5% CO_2. VSMC lineage was confirmed by immunocytochemistry using an antibody directed against α-smooth muscle actin (SMA, Sigma). Experiments with VSMCs were performed using cells that were passaged between 2–8 times.

Measurement of gene expression by quantitative RT-PCR—Total RNA from aortas and cultured cells was extracted by the phenol/guanidinium method[56]. Reverse transcription was performed using the High-Capacity cDNA Reverse Transcription Kit (Applied Biosystems, Foster City, CA, USA). A Mastercycler ep Realplex (Eppendorf, Hamburg, Germany) was used for real-time amplification and quantification of transcripts. Relative expression of target transcripts was normalized to levels of 18S ribosomal RNA, determined using the relative C_T method. Taqman® gene expression assays were used to quantify mRNA levels encoding *RUNX2*, *HDAC9*, *TNAP* and *COL3A1*.

Statistical analysis—Statistical analysis was performed using Graph Pad Prism 5.0 (GraphPad Software, La Jolla, CA) and Stata 13.0 (StataCorp LLC). The Shapiro-Wilk test was used to determine the normality of each continuous variable, and all such variables were found to be normally distributed. Data are reported as mean ± s.e.m., unless otherwise indicated. Two group comparisons of continuous variables were performed using the two-tailed Student *t* test. For more than 2 group comparisons of continuous variables, two-tailed one-way analysis of variance (ANOVA) with Sidak post-hoc testing was employed. All *in vitro* experiments were performed at least in duplicate. The Kaplan-Meier statistic with log-rank testing was used to compare survival of *Mgp*$^{-/-}$ *Hdac9*$^{-/-}$ mice and *Mgp*$^{-/-}$ *Hdac9*$^{+/+}$ mice. A two-tailed $P < 0.05$ was considered to indicate statistical significance.

Reporting summary

Further information on research design is available in the Nature Research Life Sciences Reporting Summary linked to this article.

Data availability

The summary statistics for the cohorts used in the meta-analysis and validation have been placed in dbGaP (accession phs000930), as per the policy of the CHARGE consortium[57].

The remaining data that support the findings of this study are available from the corresponding author upon request.

Supplementary Material

Refer to Web version on PubMed Central for supplementary material.

Acknowledgements

We acknowledge the essential role of the Cohorts for Heart and Aging Research in Genome Epidemiology (CHARGE) Consortium in development and support of this manuscript. The views expressed in this manuscript are those of the authors and do not necessarily represent the views of the National Heart, Lung, and Blood Institute; the National Institutes of Health; or the U. S. Department of Health and Human Services.

The Framingham Heart Study: From the Framingham Heart Study of the National Heart Lung and Blood Institute of the National Institutes of Health and Boston University School of Medicine. This work was supported by the National Heart, Lung and Blood Institute's Framingham Heart Study (Contract No. N01-HC-25195) and its contract with Affymetrix, Inc for genotyping services (Contract No. N02-HL-6-4278). R.M. was supported by the National Heart, Lung, and Blood Institute (K08HL111210 and R01HL142809), the American Heart Association (18TPA34230025), the Wild Family Foundation, and the Hassenfeld Scholar Award. F.W. was supported by Deutsche Forschungsgemeinschaft (DFG; Wu 841/1-1). A.B. was supported by the Department of Defense – Peer Reviewed Medical Research Program/Discovery Award (W81XWH-17-1-0058). C. Song was supported by an international post-doctoral fellowship from the Swedish research council (2016-00598). U.H. was supported by KOWA, MedImmune, HeartFlow, Duke University (Abbott), Oregon Health & Science University (AHA, 13FTF16450001), Columbia University (NIH, 5R01-HL109711), NIH/NHLBI 5K24HL113128, NIH/NHLBI 5T32HL076136, NIH/NHLBI 5U01HL123339. M.E.L. was supported by the Fredman Fellowship, the Toomey Fund for Aortic Dissection Research, and R01 HL130113. D.B.B. was supported by the Leducq Fondation and the National Institutes of Diabetes and Digestive and Kidney Diseases (5R01DK082971).

The Age, Gene/Environment Susceptibility-Reykjavik Study has been funded by National Institute on Aging contract N01-AG-12100 with contributions from the National Eye Institute; National Institute on Deafness and Other Communication Disorders; National Heart, Lung and Blood Institute; National Institute on Aging Intramural Research Program; Hjartavernd (the Icelandic Heart Association); and the Althingi (Icelandic Parliament).

MESA and the MESA SHARe project are conducted and supported by the National Heart, Lung, and Blood Institute (NHLBI) in collaboration with MESA investigators. MESA was supported by R01 HL071739, R01 HL72403, and by contracts HHSN268201500003I, N01-HC-95159, N01-HC-95160, N01-HC-95161, N01-HC-95162, N01-HC-95163, N01-HC-95164, N01-HC-95165, N01-HC-95166, N01-HC-95167, N01-HC-95168, N01-HC-95169, UL1-TR-000040, UL1-TR-001079, UL1-TR-001420. Funding for SHARe genotyping was provided by NHLBI Contract N02-HL-64278. Genotyping was performed at Affymetrix (Santa Clara, CA, USA) and the Broad Institute of Harvard and MIT (Boston, MA, USA) using the Affymetrix Genome-Wide Human SNP Array 6.0. This work was also supported in part by the National Center for Advancing Translational Sciences, CTSI grant UL1TR001881, and the National Institute of Diabetes and Digestive and Kidney Disease Diabetes Research Center (DRC) grant DK063491 to the Southern California Diabetes Endocrinology Research Center. M.B. was supported by the NIH. We thank the other investigators, the staff, and the participants of the MESA study for their valuable contributions. A full list of participating MESA investigators and institutions can be found at http://www.mesa-nhlbi.org.

The Family Heart Study (FamHS) research was supported by NIH grants: R01-HL-117078 from NHLBI, and R01-DK-089256 from NIDDK.

We are indebted to all the study participants and to the dedicated personnel of both the study center of the Heinz Nixdorf Recall study and the EBT-scanner facilities D. Grönemeyer, Bochum, and R. Seibel, Mülheim, as well as to the investigative group, in particular to U. Roggenbuck, U. Slomiany, E. M. Beck, A. Öffner, S. Münkel, M. Bauer, S. Schrader, R. Peter, and H. Hirche. **Scientific advisory board:** T. Meinertz, Hamburg (Chair); M. Blettner, Mainz; C. Bode, Freiburg; P. J. de Feyter, Rotterdam, Zürich, Niederlande; B. Güntert, Hall i.T., Schweiz; F. Gutzwiller, Schweiz; H. Heinen, Bonn; O. Hess (deceased), Bern, Schweiz; B. Klein (deceased), Essen; H. Löwel, Neuherberg; M. Reiser, München; G. Schmidt (deceased), Essen; M. Schwaiger, München; C. Steinmüller, Bonn; T. Theorell, Stockholm, Schweden; S. N. Willich, Berlin. **Criteria and end point committee:** C. Bode, Freiburg (Chair), K. Berger, Münster; H. R. Figulla, Jena; C. Hamm, Bad Nauheim; P. Hanrath, Aachen; W. Köpcke, Münster; C. Weimar, Essen; A. Zeiher, Frankfurt. **Funding:** We thank the Heinz Nixdorf Foundation (Chairman: M. Nixdorf; Past Chairman: G. Schmidt (deceased)), the German Ministry of Education and Science (BMBF) and the "Deutsche Forschungsgemeinschaft" (Project numbers: ER 155/6-1 and ER 155/6-2) for the generous support

of this study. An additional research grant was received from Imatron Inc., South San Francisco, CA, which produced the EBCT scanners, and GE-Imatron, South San Francisco, CA, after the acquisition of Imatron Inc. We acknowledge the support of the Sarstedt AG & Co. (Nümbrecht, Germany) concerning laboratory equipment. We received a generous support from the Ministry of Culture and Science of North Rhine-Westphalia and the Faculty of Medicine University Duisburg-Essen for the genotyping of the Heinz Nixdorf Recall study participants. S.P. was supported by the "Deutsche Forschungsgemeinschaft" (Project No.: PE 2309/2-1). Technical support for the imputation of the Heinz Nixdorf Recall Study data on the Supercomputer Cray XT6m was provided by the Center for Information and Media Services, University of Duisburg-Essen.

The African American-Diabetes Heart Study (AA-DHS) was supported by NIH grants: R01-DK-071891 from NIDDK, RO1-HL-67348 from NHLBI, and General Clinical Research Center of Wake Forest School of Medicine M01-RR-07122.

N.F. is supported by the following NIH grants: MD012765, DK117445, and HL140385.

References

1. Greenland P, LaBree L, Azen SP, Doherty TM & Detrano RC Coronary artery calcium score combined with Framingham score for risk prediction in asymptomatic individuals. JAMA 291, 210–5 (2004). [PubMed: 14722147]
2. Budoff MJ et al. Assessment of coronary artery disease by cardiac computed tomography: a scientific statement from the American Heart Association Committee on Cardiovascular Imaging and Intervention, Council on Cardiovascular Radiology and Intervention, and Committee on Cardiac Imaging, Council on Clinical Cardiology. Circulation 114, 1761–91 (2006). [PubMed: 17015792]
3. O'Donnell CJ et al. Genome-wide association study for coronary artery calcification with follow-up in myocardial infarction. Circulation 124, 2855–64 (2011). [PubMed: 22144573]
4. Natarajan P et al. Multiethnic Exome-Wide Association Study of Subclinical Atherosclerosis. Circ Cardiovasc Genet 9, 511–520 (2016). [PubMed: 27872105]
5. Thanassoulis G et al. Genetic associations with valvular calcification and aortic stenosis. N Engl J Med 368, 503–12 (2013). [PubMed: 23388002]
6. Post W et al. Determinants of coronary artery and aortic calcification in the old order amish. Circulation 115, 717–724 (2007). [PubMed: 17261661]
7. Criqui MH et al. Abdominal aortic calcium, coronary artery calcium, and cardiovascular morbidity and mortality in the Multi-Ethnic Study of Atherosclerosis. Arterioscler Thromb Vasc Biol 34, 1574–9 (2014). [PubMed: 24812323]
8. Budoff MJ et al. Thoracic aortic calcification and coronary heart disease events: the multi-ethnic study of atherosclerosis (MESA). Atherosclerosis 215, 196–202 (2011). [PubMed: 21227418]
9. Bastos Goncalves F et al. Calcification of the abdominal aorta as an independent predictor of cardiovascular events: a meta-analysis. Heart 98, 988–94 (2012). [PubMed: 22668866]
10. Wilson PW et al. Abdominal aortic calcific deposits are an important predictor of vascular morbidity and mortality. Circulation 103, 1529–34 (2001). [PubMed: 11257080]
11. Erbel R et al. 2014 ESC Guidelines on the diagnosis and treatment of aortic diseases: Document covering acute and chronic aortic diseases of the thoracic and abdominal aorta of the adult. The Task Force for the Diagnosis and Treatment of Aortic Diseases of the European Society of Cardiology (ESC). Eur Heart J 35, 2873–926 (2014). [PubMed: 25173340]
12. Guerin AP, London GM, Marchais SJ & Metivier F Arterial stiffening and vascular calcifications in end-stage renal disease. Nephrol Dial Transplant 15, 1014–21 (2000). [PubMed: 10862640]
13. London GM Mechanisms of arterial calcifications and consequences for cardiovascular function. Kidney Int Suppl (2011) 3, 442–445 (2013). [PubMed: 25019027]
14. Sigrist MK, Taal MW, Bungay P & McIntyre CW Progressive vascular calcification over 2 years is associated with arterial stiffening and increased mortality in patients with stages 4 and 5 chronic kidney disease. Clin J Am Soc Nephrol 2, 1241–8 (2007). [PubMed: 17928470]
15. Psaty BM et al. Cohorts for Heart and Aging Research in Genomic Epidemiology (CHARGE) Consortium: Design of prospective meta-analyses of genome-wide association studies from 5 cohorts. Circ Cardiovasc Genet 2, 73–80 (2009). [PubMed: 20031568]

16. Yang J et al. Genomic inflation factors under polygenic inheritance. Eur J Hum Genet 19, 807–12 (2011). [PubMed: 21407268]
17. Nikpay M et al. A comprehensive 1,000 Genomes-based genome-wide association meta-analysis of coronary artery disease. Nat Genet 47, 1121–30 (2015). [PubMed: 26343387]
18. Markus HS et al. Evidence HDAC9 genetic variant associated with ischemic stroke increases risk via promoting carotid atherosclerosis. Stroke 44, 1220–5 (2013). [PubMed: 23449258]
19. Franceschini N et al. GWAS and colocalization analyses implicate carotid intima-media thickness and carotid plaque loci in cardiovascular outcomes. Nat Commun 9, 5141 (2018). [PubMed: 30510157]
20. Bellenguez C et al. Genome-wide association study identifies a variant in HDAC9 associated with large vessel ischemic stroke. Nat Genet 44, 328–33 (2012). [PubMed: 22306652]
21. Foroud T et al. Genome-wide association study of intracranial aneurysm identifies a new association on chromosome 7. Stroke 45, 3194–9 (2014). [PubMed: 25256182]
22. Ramos EM et al. Phenotype-Genotype Integrator (PheGenI): synthesizing genome-wide association study (GWAS) data with existing genomic resources. Eur J Hum Genet 22, 144–7 (2014). [PubMed: 23695286]
23. Grunstein M Histone acetylation in chromatin structure and transcription. Nature 389, 349–52 (1997). [PubMed: 9311776]
24. Haberland M, Montgomery RL & Olson EN The many roles of histone deacetylases in development and physiology: implications for disease and therapy. Nat Rev Genet 10, 32–42 (2009). [PubMed: 19065135]
25. Chang S et al. Histone deacetylases 5 and 9 govern responsiveness of the heart to a subset of stress signals and play redundant roles in heart development. Mol Cell Biol 24, 8467–76 (2004). [PubMed: 15367668]
26. Lobera M et al. Selective class IIa histone deacetylase inhibition via a nonchelating zinc-binding group. Nat Chem Biol 9, 319–25 (2013). [PubMed: 23524983]
27. Rusanescu G, Weissleder R & Aikawa E Notch signaling in cardiovascular disease and calcification. Curr Cardiol Rev 4, 148–56 (2008). [PubMed: 19936191]
28. Leopold JA Vascular calcification: Mechanisms of vascular smooth muscle cell calcification. Trends Cardiovasc Med 25, 267–74 (2015). [PubMed: 25435520]
29. Ngo P, Ramalingam P, Phillips JA & Furuta GT Collagen gel contraction assay. Methods Mol Biol 341, 103–9 (2006). [PubMed: 16799192]
30. Luo G et al. Spontaneous calcification of arteries and cartilage in mice lacking matrix GLA protein. Nature 386, 78–81 (1997). [PubMed: 9052783]
31. Kato N et al. Trans-ancestry genome-wide association study identifies 12 genetic loci influencing blood pressure and implicates a role for DNA methylation. Nature genetics 47, 1282–93 (2015). [PubMed: 26390057]
32. McEniery CM et al. Aortic calcification is associated with aortic stiffness and isolated systolic hypertension in healthy individuals. Hypertension 53, 524–31 (2009). [PubMed: 19171791]
33. Paultre F & Mosca L Association of blood pressure indices and stroke mortality in isolated systolic hypertension. Stroke 36, 1288–90 (2005). [PubMed: 15879322]
34. Schurgers LJ, Uitto J & Reutelingsperger CP Vitamin K-dependent carboxylation of matrix Gla-protein: a crucial switch to control ectopic mineralization. Trends Mol Med 19, 217–26 (2013). [PubMed: 23375872]
35. Nigwekar SU et al. Vitamin K-Dependent Carboxylation of Matrix Gla Protein Influences the Risk of Calciphylaxis. J Am Soc Nephrol 28, 1717–1722 (2017). [PubMed: 28049648]
36. Steitz SA et al. Smooth muscle cell phenotypic transition associated with calcification: upregulation of Cbfa1 and downregulation of smooth muscle lineage markers. Circ Res 89, 1147–54 (2001). [PubMed: 11739279]
37. Sun Y et al. Smooth muscle cell-specific runx2 deficiency inhibits vascular calcification. Circ Res 111, 543–52 (2012). [PubMed: 22773442]

38. Brozovich FV et al. Mechanisms of Vascular Smooth Muscle Contraction and the Basis for Pharmacologic Treatment of Smooth Muscle Disorders. Pharmacol Rev 68, 476–532 (2016). [PubMed: 27037223]
39. Lino Cardenas CL et al. An HDAC9-MALAT1-BRG1 complex mediates smooth muscle dysfunction in thoracic aortic aneurysm. Nat Commun 9, 1009 (2018). [PubMed: 29520069]
40. Agatston AS et al. Quantification of coronary artery calcium using ultrafast computed tomography. J Am Coll Cardiol 15, 827–32 (1990). [PubMed: 2407762]
41. Rumberger JA & Kaufman L A rosetta stone for coronary calcium risk stratification: agatston, volume, and mass scores in 11,490 individuals. AJR Am J Roentgenol 181, 743–8 (2003). [PubMed: 12933474]
42. Budoff MJ et al. Effect of scanner type on the reproducibility of extracoronary measures of calcification: the multi-ethnic study of atherosclerosis. Acad Radiol 14, 1043–9 (2007). [PubMed: 17707311]
43. Budoff MJ et al. Reproducibility of CT measurements of aortic valve calcification, mitral annulus calcification, and aortic wall calcification in the multi-ethnic study of atherosclerosis. Acad Radiol 13, 166–72 (2006). [PubMed: 16428051]
44. Chuang ML et al. Distribution of abdominal aortic calcium by computed tomography: impact of analysis method on quantitative calcium score. Acad Radiol 20, 1422–8 (2013). [PubMed: 24119355]
45. Willer CJ, Li Y & Abecasis GR METAL: fast and efficient meta-analysis of genomewide association scans. Bioinformatics 26, 2190–1 (2010). [PubMed: 20616382]
46. Zhang X et al. Identification of common genetic variants controlling transcript isoform variation in human whole blood. Nat Genet 47, 345–52 (2015). [PubMed: 25685889]
47. Zhang CL et al. Class II histone deacetylases act as signal-responsive repressors of cardiac hypertrophy. Cell 110, 479–88 (2002). [PubMed: 12202037]
48. O'Rourke C et al. Calcification of Vascular Smooth Muscle Cells and Imaging of Aortic Calcification and Inflammation. J Vis Exp (2016).
49. Kang H et al. Bone morphogenetic protein 4 promotes vascular smooth muscle contractility by activating microRNA-21 (miR-21), which down-regulates expression of family of dedicator of cytokinesis (DOCK) proteins. The Journal of biological chemistry 287, 3976–86 (2012). [PubMed: 22158624]
50. Aikawa E et al. Osteogenesis associates with inflammation in early-stage atherosclerosis evaluated by molecular imaging in vivo. Circulation 116, 2841–50 (2007). [PubMed: 18040026]
51. Aikawa E et al. Multimodality molecular imaging identifies proteolytic and osteogenic activities in early aortic valve disease. Circulation 115, 377–86 (2007). [PubMed: 17224478]
52. Malhotra R et al. Inhibition of bone morphogenetic protein signal transduction prevents the medial vascular calcification associated with matrix Gla protein deficiency. PLoS One 10, e0117098 (2015). [PubMed: 25603410]
53. Malhotra R et al. Hepcidin Deficiency Protects Against Atherosclerosis. Arterioscler Thromb Vasc Biol 39, 178–187 (2019). [PubMed: 30587002]
54. Derwall M et al. Inhibition of bone morphogenetic protein signaling reduces vascular calcification and atherosclerosis. Arterioscler Thromb Vasc Biol 32, 613–22 (2012). [PubMed: 22223731]
55. Rong JX, Shapiro M, Trogan E & Fisher EA Transdifferentiation of mouse aortic smooth muscle cells to a macrophage-like state after cholesterol loading. Proc Natl Acad Sci U S A 100, 13531–6 (2003). [PubMed: 14581613]
56. Chomczynski P & Sacchi N Single-step method of RNA isolation by acid guanidinium thiocyanate-phenol-chloroform extraction. Anal. Biochem. 162, 156–9 (1987). [PubMed: 2440339]
57. Rich SS et al. Rapid evaluation of phenotypes, SNPs and results through the dbGaP CHARGE Summary Results site. Nat Genet 48, 702–3 (2016). [PubMed: 27350599]

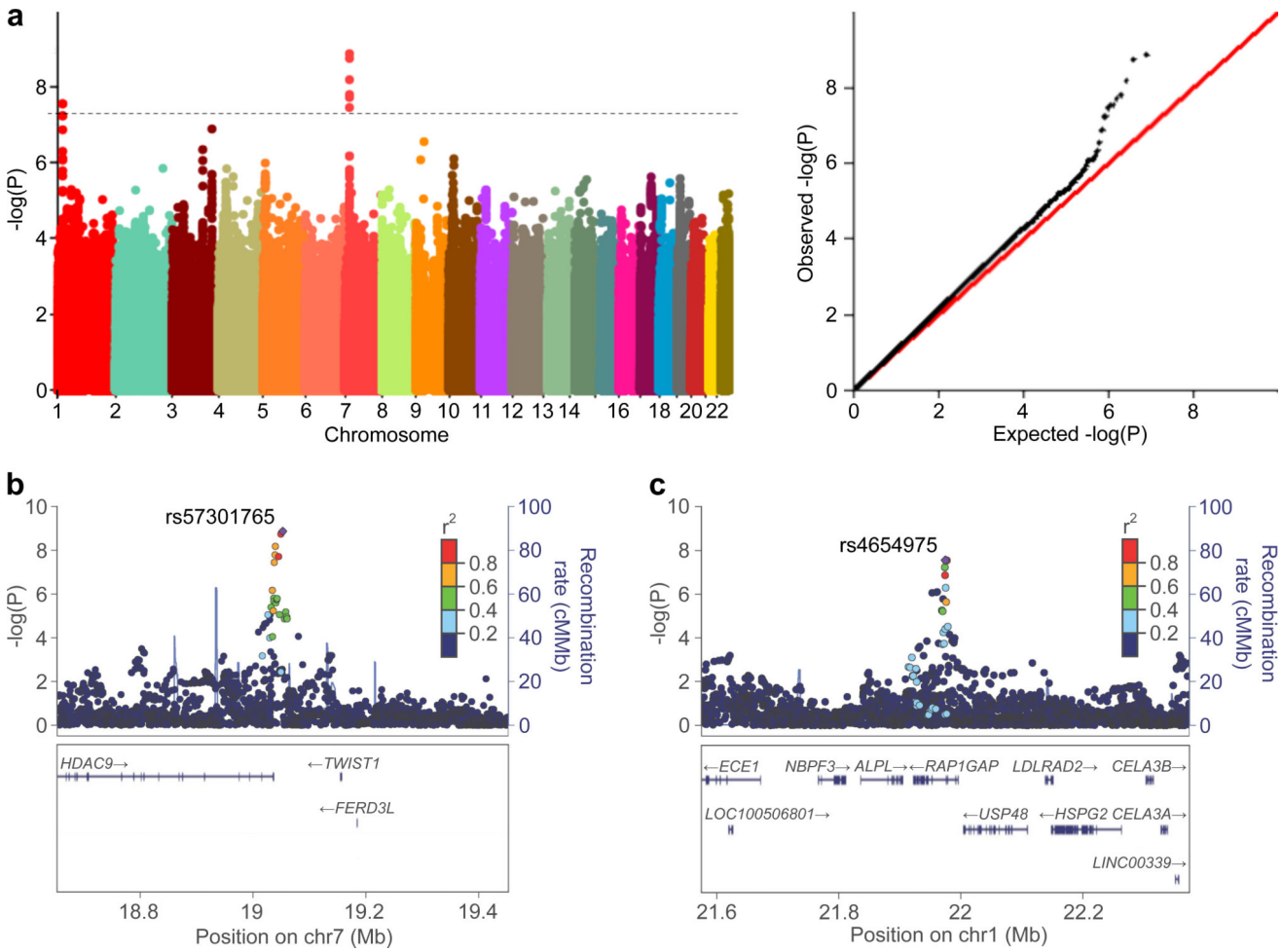

Figure 1 |. Polymorphisms in the *HDAC9* and *RAP1GAP* loci are associated with abdominal aortic calcification.

a, Manhattan (left) and Quantile-Quantile (right) plots for the association of abdominal aortic calcification with ~9 million SNPs in the GWAS meta-analysis of 9,417 participants. The hashed line indicates the genome-wide threshold for significance ($P < 5 \times 10^{-8}$). **b**, Regional SNP association map of the *HDAC9* genetic region on chromosome 7 observed in the GWAS meta-analysis, centered around the lead SNP rs57301765. **c**, Regional association map of the *RAP1GAP* genetic region on chromosome 1, centered around the lead SNP rs4654975.

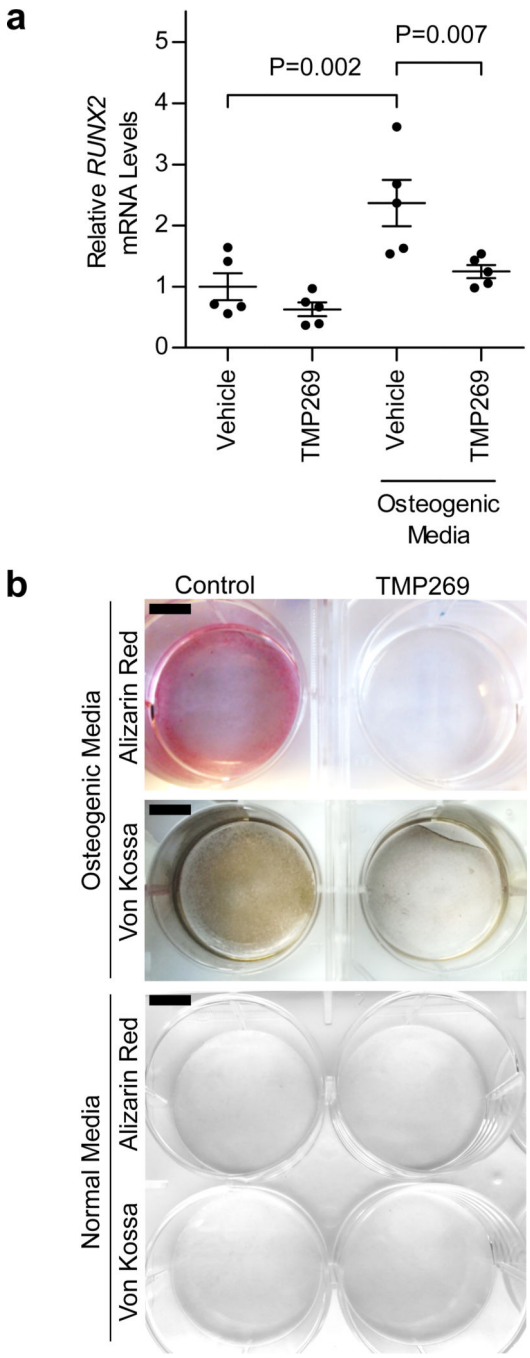

Figure 2 |. Inhibition of class IIa HDAC activity prevents osteogenic phenotype switch and calcification of cultured vascular smooth muscle cells.

HASMCs were grown in normal or osteogenic media (see Methods) in the presence or absence of TMP269 (100 nM) for either 6 or 10 days and harvested for gene expression analysis and calcification assessment, respectively. **a**, Treatment with calcification media increased *RUNX2* mRNA levels (an important regulator of osteogenic phenotype switch) in HASMCs >2-fold. However, treatment with the HDAC inhibitor TMP269 prevented this increase in *RUNX2* expression ($n = 5$ biologically independent samples for each group).

Statistical comparisons were made using a two-tailed one-way ANOVA with Sidak's test for multiple comparisons. Mean ± s.e.m. is depicted. **b**, Treatment of HASMCs with calcification media for 10 days resulted in calcification, as evidenced by Alizarin Red and von Kossa staining. Calcification of HASMCs was inhibited by TMP269. Two independent experiments were performed with representative images shown. Scale bar, 1 cm.

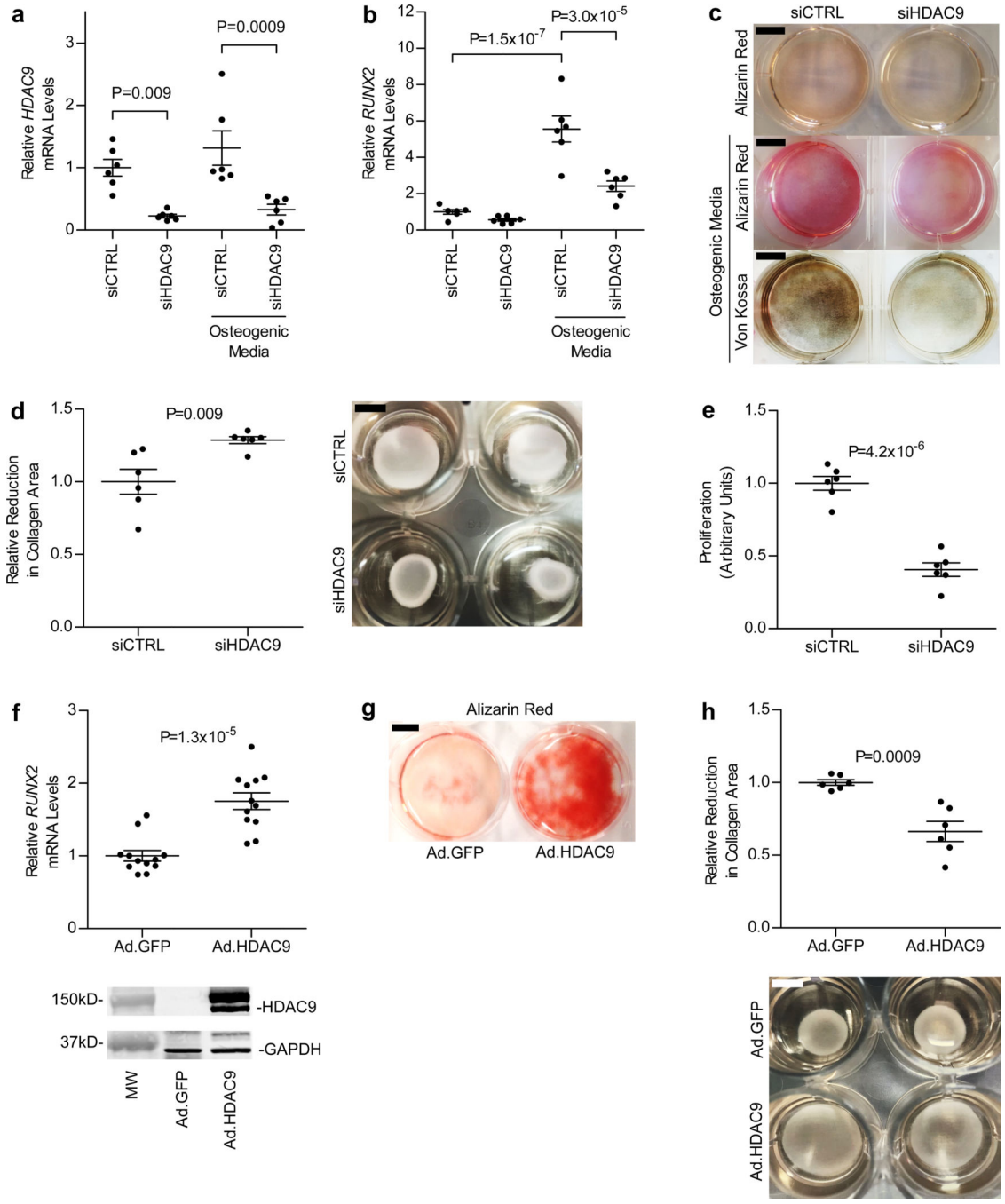

Figure 3 |. Vascular smooth muscle cell calcification, *RUNX2* expression, proliferation, and contractility are affected by changes in HDAC9 expression.

a-c, Treatment of HASMCs ($n = 6$ biologically independent samples in each group) grown in osteogenic media with siHDAC9 (resulting in >75% knockdown of *HDAC9* mRNA) (**a**) reduced *RUNX2* mRNA levels by >50% (**b**) and prevented calcification, as evidenced by decreased Alizarin Red and von Kossa staining (**c**). In **a** and **b**, statistical comparisons were made using a two-tailed one-way ANOVA with Sidak's test for multiple comparisons. In **c**, three independent experiments were performed with representative images shown. **d**,

Reduced *HDAC9* expression in HASMCs grown in collagen discs (right panel) resulted in a ~30% increase in contraction (left panel, $n = 6$ biologically independent samples in each group). **e**, Treatment of HASMCs with 20 nM siHDAC9 resulted in a 60% reduction in proliferation ($n = 6$ biologically independent samples in each group). **f**, Adenoviral expression of the 125-kDa isoform of HDAC9 fused to GFP in HASMCs was associated with a 75% increase in *RUNX2* mRNA levels, when cells were harvested 8 days after viral transduction ($n = 12$ biologically independent samples in each group). Increased expression of HDAC9 was confirmed by Western blot (lower panel) using antibodies directed against HDAC9 and GAPDH (for a loading control). A full scan of the blot is in Supplementary Figure 4a. g, As shown by Alizarin Red staining, increased HDAC9 expression resulted in augmented calcification in HASMCs. Two independent experiments were performed with representative images shown. **h**, Increased HDAC9 expression also caused a 34% decrease (left panel, $n = 6$ biologically independent samples in each group) in contraction of HASMCs grown in collagen discs (right panel). In **d**-**f** and **h**, statistical comparisons were made using a two-tailed Student *t* test. Mean ± s.e.m. is depicted in all plots. For **c** and **g**, scale bar is 1 cm. For **d** and **h**, scale bar is 0.5 cm.

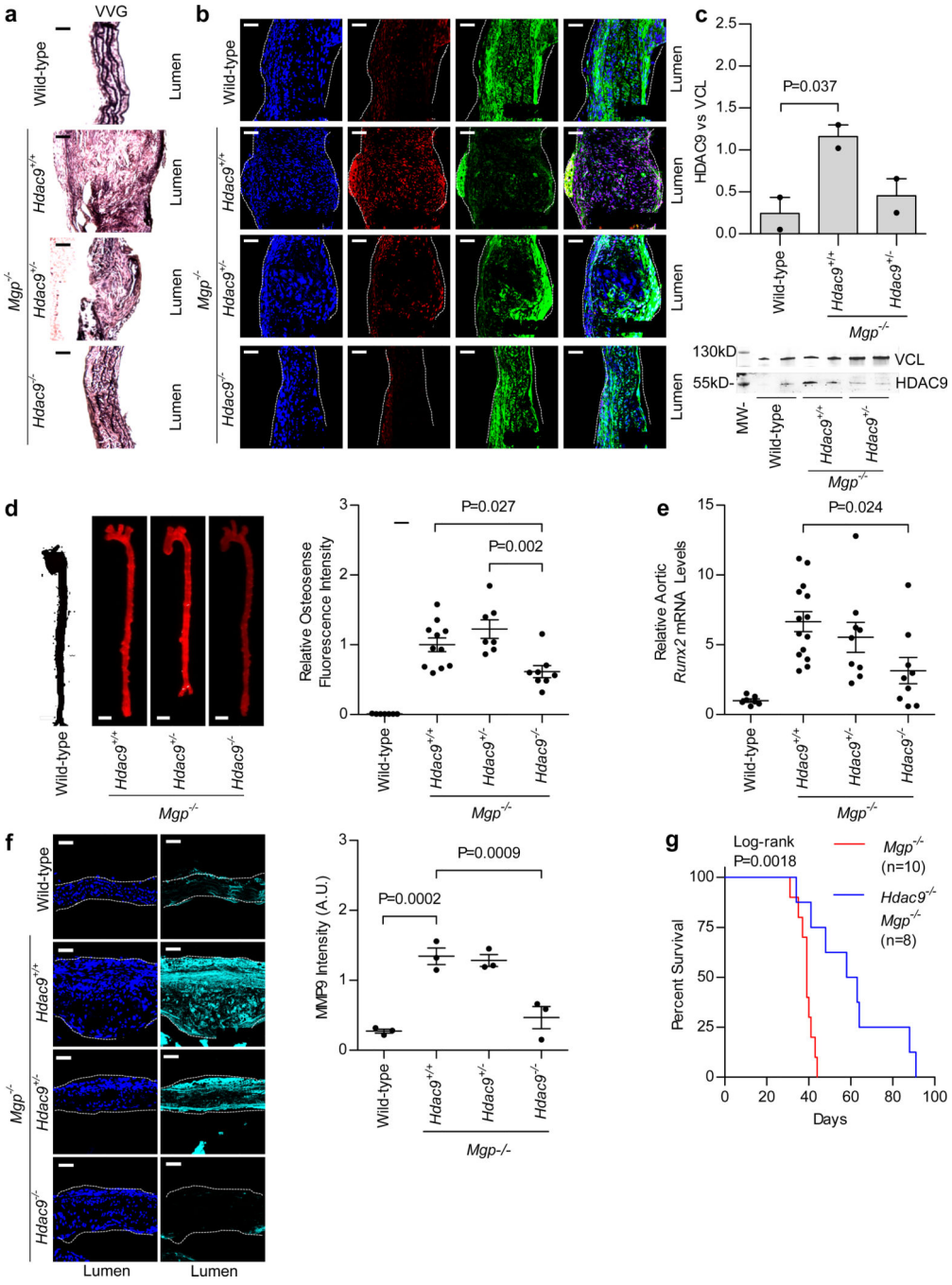

Figure 4 |. HDAC9 deficiency protects against the development of vascular calcification and aortic elastin disruption and improves survival in *Mgp*$^{-/-}$ mice.

a, Longitudinal sections of aortas stained with Verhoeff-Van Gieson (VVG) are depicted, showing elastin fiber integrity in the aortas of wild-type, *Mgp*$^{-/-}$ *Hdac9*$^{+/+}$, *Mgp*$^{-/-}$ *Hdac9*$^{+/-}$, and *Mgp*$^{-/-}$ *Hdac9*$^{-/-}$ mice. The disruption of elastin fiber integrity seen with MGP deficiency was improved with HDAC9 deficiency. **b**, Longitudinal sections of aortas isolated from 14-day-old wild-type, *Mgp*$^{-/-}$ *Hdac9*$^{+/+}$, *Mgp*$^{-/-}$ *Hdac9*$^{+/-}$, and *Mgp*$^{-/-}$ *Hdac9*$^{-/-}$ mice were stained for HDAC9 (red), SM22α (green, a contractile protein), and

DNA (blue, DAPI). Increased levels of HDAC9 protein were seen in *Mgp*$^{-/-}$ *Hdac9*$^{+/+}$ aortas, and to an intermediate degree in *Mgp*$^{-/-}$ *Hdac9*$^{+/-}$ aortas, relative to wild-type aortas. HDAC9 localized primarily to nuclei. Increased HDAC9 expression was associated with reduced SM22α expression. In **a** and **b**, three independent replicates in each group were assessed with representative images shown. **c**, Western blot of proteins isolated from aortas of wild-type, *Mgp*$^{-/-}$ *Hdac9*$^{+/+}$, and *Mgp*$^{-/-}$ *Hdac9*$^{+/-}$ mice (n = 2 mice in each group) confirmed increased levels of the 50-kDa isoform of HDAC9 protein in *Mgp*$^{-/-}$ *Hdac9*$^{+/+}$ mice and to a lesser extent in *Mgp*$^{-/-}$ *Hdac9*$^{+/-}$ mice compared to wild-type mice. Statistical comparison was made using a two-tailed one-way ANOVA with Sidak's test. A full scan of the blot is shown in Supplementary Figure 4b. d, Aortic calcification, as assessed by OsteoSense near-infrared imaging (left panel), was reduced by ~40–50% (right panel) in 21-day-old mice that were deficient in both MGP and HDAC9 (*Mgp*$^{-/-}$ *Hdac9*$^{-/-}$, n = 8) compared to *Mgp*$^{-/-}$ *Hdac9*$^{+/+}$ mice (n = 11) and *Mgp*$^{-/-}$ *Hdac9*$^{+/-}$ (n = 7) mice. No aortic calcification was observed in wild-type mice (n = 7). Scale bar is 1 mm. **e**, *Mgp*$^{-/-}$ *Hdac9*$^{+/+}$ mice (n = 14) had increased aortic *Runx2* mRNA levels compared to wild-type mice (n = 7, P < 0.0001). Compared to *Mgp*$^{-/-}$ *Hdac9*$^{+/+}$ mice, *Mgp*$^{-/-}$ *Hdac9*$^{-/-}$ mice (n = 9) had a ~50% reduction in aortic *Runx2* mRNA levels (P = 0.024). **f**, Immunofluorescence with an antibody directed against MMP9 demonstrated a >60% reduction of MMP9 expression in aortic sections from HDAC9-deficient *Mgp*$^{-/-}$ mice when compared to *Mgp*$^{-/-}$ *Hdac9*$^{+/+}$ and *Mgp*$^{-/-}$ *Hdac9*$^{+/-}$ mice (n = 3 mice in each group). DAPI (dark blue) was used as a nuclear stain. In **d-f**, statistical comparisons were made using a two-tailed one-way ANOVA with Sidak's test for multiple comparisons. **g**, Improved Kaplan-Meier survival was observed in *Mgp*$^{-/-}$ *Hdac9*$^{-/-}$ mice (n = 8) compared to *Mgp*$^{-/-}$ *Hdac9*$^{+/+}$ mice (n = 10, two-sided log-rank P = 0.0018). For **a**, **b**, and **f**, scale bar is 50 μm. Mean ± s.e.m. is depicted in all plots.

Table 1 |

Genome-wide significant and near-significant SNPs associated with abdominal aortic calcification and thoracic aortic calcification from discovery-stage meta-analysis

SNP	Chromosome	Minor allele	MAF	*Z* score	*P*-value	Direction of effect	No. studies	Imputation score	Nearest gene(s)
Abdominal aortic calcification (continuous trait)									
rs57301765	7	A	0.17	6.07	1.3×10^{-9}	+ + + +	4	0.957	*HDAC9*
rs2107595	7	A	0.17	6.02	1.7×10^{-9}	+ + + +	4	0.970	*HDAC9*
rs28688791	7	C	0.20	5.80	6.5×10^{-9}	+ + + +	4	0.978	*HDAC9*
rs2023936	7	G	0.20	5.65	1.6×10^{-8}	+ + + +	4	0.992	*HDAC9*
rs2526620	7	G	0.21	5.62	1.9×10^{-8}	+ + + +	4	0.904	*HDAC9*
rs4654975	1	C	0.34	5.55	2.8×10^{-8}	+ + + +	4	0.936	*RAP1GAP*
rs3767120	1	C	0.33	5.55	2.8×10^{-8}	+ + + +	4	0.891	*RAP1GAP*
rs7798197	7	G	0.20	5.51	3.5×10^{-8}	+ + + +	4	0.995	*HDAC9*
Thoracic aortic calcification (continuous trait)									
rs58674255	9	C	0.23	5.35	8.6×10^{-8}	+ + + +	4	0.997	*VPS13A*

Single SNP association test was performed by each cohort using two-sided multivariate linear regression, adjusting for age, sex, study sites when appropriate, and top principal components. GWAS results from all cohorts were meta-analyzed using sample size weighted fixed-effect models as implemented in the program METAL. A genome-wide significance threshold of 5×10^{-8} was used in consideration of multiple comparisons in GWAS. Abbreviations: SNP, single nucleotide polymorphism; MAF, minor allele frequency; No. studies, number of studies.

Table 2 |

Trans-ethnic replication of genome-wide significant SNPs for abdominal aortic calcification in Hispanic Americans in MESA

Hispanic Americans (*n* = 496)					
SNP	**Chromosome**	**Minor allele**	**MAF**	***Z* score**	***P*-value**
rs57301765	7	A	0.26	4.12	3.8×10^{-5}
rs2107595	7	A	0.25	4.69	2.8×10^{-6}
rs28688791	7	C	0.27	4.49	7.1×10^{-6}
rs2023936	7	G	0.29	3.73	1.9×10^{-4}
rs2526620	7	G	0.31	4.16	3.2×10^{-5}
rs7798197	7	G	0.29	4.13	3.6×10^{-5}
rs4654975	1	C	0.41	1.47	0.14
rs3767120	1	C	0.44	1.31	0.19

Single SNP association test was performed by each cohort using two-sided multivariate linear regression, adjusting for age, sex, study sites when appropriate, and top principal components. To adjust for multiple testing, we applied Bonferroni corrections, i.e. $P < 0.05/6$ for *HDAC9,* and $P < 0.05/2$ for *RAP1GAP.*